J. Nano- Electron. Phys.
3 (2011) No1, P. 868-877

PACS numbers: 85.60. – q, 71.55.Eq

A TWO-DIMENSIONAL (2D) POTENTIAL DISTRIBUTION MODEL FOR THE SHORT GATE-LENGTH ION-IMPLANTED GaAs MESFETs UNDER DARK AND ILLUMINATED CONDITIONS

Shweta Tripathi, S. Jit

[1] Centre for Research in Microelectronics (CRME), Department of Electronics Engineering, Institute of Technology,
Banaras Hindu University, 221005, Varanasi, India
E-mail: sjit.ece@itbhu.ac.in

An analytical 2D model to predict the potential distribution of short-channel ion-implanted GaAs MESFETs has been presented. The 2D potential distribution in the channel of the short-channel device has been obtained by solving the 2D Poisson's equation in conjunction with suitable boundary conditions using superposition method. The remarkable feature of the proposed model is that the implanted doping profile has been treated in completely analytical manner. A double-integrable Gaussian-like function has been assumed as the doping distribution profile in the vertical direction of the channel. The effects of excess carrier generation due to the incident optical radiation in channel region have been included in the Poisson's equation to study the optical effects on the device. The photovoltage developed across the gate metal has also been modeled. The proposed model has been verified by comparing the theoretically predicted results with simulated data obtained by using the commercially available ATLAS^{TM}2D device simulator.

Keywords: *SHORT CHANNEL GaAs MESFET, ION-IMPLANTATION, OPTICAL BIASING, POISSON'S EQUATION, PHOTOVOLTAGE.*

(Received 04 February 2011)

1. INTRODUCTION

GaAs Metal-Semiconductor Field Effect Transistors (GaAs MESFETs) have drawn considerable attention for the designing of high-speed digital/analog integrated circuits and microwave monolithic ICs [1-6]. When the light is incident on the transparent/semi-transparent gate of the device excess electron-hole pairs are generated in the channel due to the incident optical radiation which can be utilized to control the device characteristics. Since these excess electron-hole pairs can be controlled by the radiated power level of the external optical source, the radiated power level has direct control on the device characteristics. The optical radiation incident on the device can thus be viewed as an extra input terminal of the MESFET through which the microwave device or circuit (e.g. MMIC) performance can be governed[7].

Optically controlled microwave devices and systems exhibit certain advantages such as size reduction, signal isolation, large bandwidth and immunity to electromagnetic interference. It has also been shown that the incident illumination reduces the noise figure but increases the unilateral power gain of a GaAs OPFET [8-9]. Due to such properties, high-speed, low-cost, monolithically integrated optically gated GaAs MESFETs are presently in high demand for low-wavelength high-frequency optical communication systems [7, 10].

Analytical models are generally limited by the mathematical treatment when multidimensional geometry is considered. The complexity is increased further if the modeling is carried out for device operating under illuminated condition where the additional effects of incident illumination on the device characteristics are required to be included in the model. A number of investigations [11-15] have been reported to study the photo effects on potential distribution of GaAs-MESFET to describe its operation and application under dark and illuminated conditions. A closed form analytical model of an optically controlled Si-MESFET was proposed by Singh et al. [11]. The model was later extended by Mishra et al. [12] for a GaAs OPFET. They considered the main contribution of the optically generated carriers to be photoconductive in nature. Chakrabarti et al. [13] later modified this model and included gate photovoltaic effect. All the above mentioned models lacks the short geometry effects and account only for the long channel MESFET device under illumination. Taking this into account, Bose et al. [14] later presented a potential distribution and threshold voltage model for uniformly doped GaAs MESFETs under illuminated condition by solving the 2D Poisson's equation. Mishra et al. [15] presented two-dimensional (2D) numerical model of non-uniformly doped MESFET under illumination using Monte Carlo finite difference method. However, a number of works have been reported for the modeling of potential distribution of optically biased GaAs MESFETs. To the best of our knowledge, no work has been reported so far in the literature for the analysis of potential distribution of ion-implanted short-channel GaAs MESFETs under dark and illuminated condition considering optical carrier generation and recombination effects.

When optical illumination is incident, due to generation of carriers in the channel, there is an increase in the drain saturation current that can be increased further by the non-uniform heavily doped channel region [16]. In general, number of techniques are there to produce non-uniform doping profile techniques among those techniques ion-implantation is the effective one for improved GaAs MESFET performance [17]. Since ion-implanted technique produces Gaussian doping profile that can not be integrated analytically within finite limits hence in the present analysis Gaussian-like analytic function proposed by Dasgupta et al. [18], has been used in place of actual Gaussian function to represent doping profile in the channel.

In the present paper an effort has been made to analytically model the channel potential distribution of the short channel optically biased GaAs MESFETs .The 2D potential distribution in the channel of the short-channel device has been obtained by solving the 2D Poisson's equation with suitable boundary conditions. Photoeffects have been included by incorporating proper parameters in the Poisson's equation. The photovoltage developed across the gate metal has also been modeled for the Gaussian doped channel. The theoretically predicted results are compared with the numerical sy-axis. Indium Tin Oxide (ITO) has been used as the Schottky-gate metal due to its high optical transmittance of incident illumination on its gate surface [20]. An undoped high pure LEC semi-insulating GaAs material is assumed as substrate of the device. The active channel region of the device is an n-GaAs layer which can be obtained by ion implanting Si into semi-insulating substrate.

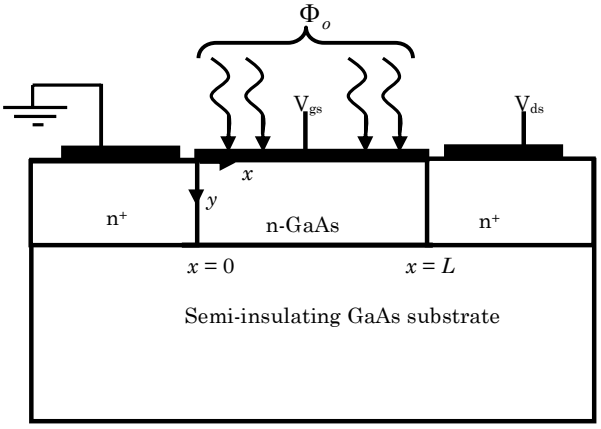

Fig. 1 *– Schematic diagram of a GaAs MESFET where, L and a are the channel length and thickness respectively*

The ion-implanted profile in the channel region can be given as [21]

$$N(y) = \frac{Q}{\sigma\sqrt{2\pi}} \exp\left[-\left(\frac{y - R_p}{\sigma\sqrt{2}}\right)^2\right] = N_p \exp\left[-\left(\frac{y - R_p}{\sigma\sqrt{2}}\right)^2\right] \quad (1)$$

where Q is the dose, R_p is the projected range, σ is the projected straggle, and $N_p = Q/\sigma\sqrt{2\pi}$ is peak ion concentration in the substrate.

If the undoped substrate is assumed to have a uniform doping concentration of N_s, the doping distribution in the channel can approximately be described by [22]

$$N_d(y) = N_s + (N_p - N_s) \exp\left[-\left(\frac{y - R_p}{\sigma\sqrt{2}}\right)^2\right] = N_s + (N_p - N_s)F(y) \quad (2)$$

where $N_d(y)$ is an analytically non-integrable function of y because of the exponential function $F(y)$. Therefore, we have used an approximate analytic form of $F(y)$ as [18]

$$F(y) \approx c_c \left[\left\{a_c + \frac{2b_c\beta}{\sqrt{2}\,\sigma}(y - R_p)\right\}^2 - 2b_c\right] \exp\left[-\left\{\frac{a_c\beta}{\sqrt{2}\sigma}(y - R_p) + \frac{b_c}{2\sigma^2}(y - R_p)^2\right\}\right] \quad (3)$$

where $a_c = 1.7857142$, $b_c = 0.6460853$, $c_c = 0.24857142\sqrt{\pi}$ and $\beta = +1$ for $y > R_p$ $\beta = -1$ for $y < R_p$. Now, the net doping concentration $N_D(y)$ in the active channel region under illuminated condition which can be given as [23]

$$N_D(y) = N_d(y) + G(y)\tau_n - \frac{R\tau_p}{a} \quad (4)$$

where $N_d(y)$ represents the doping profile defined by Eq.(2). R is the surface recombination rate, α is the absorption coefficient of GaAs material, τ_n and τ_p are the life time of electrons and holes, respectively and $G(y)$ is the photo-generation rate given as Ref. [21].

When the illumination is incident on the gate metal of the GaAs MESFET device a photovoltage is developed across the gate given as [24]

$$V_{op} = \frac{nkT}{q} \ln\left(1 + \frac{J_p(0)}{J_s}\right). \tag{5}$$

Following the methodology used in Ref. [24] hole current density at the gate-channel interface $J_p(0)$ has been obtained as

$$J_p(0) = q v_p \; p_d(y)\big|_{y=0}, \tag{6}$$

where v_p is the saturation velocity of hole and $p_p(y)$ is the hole density in the depletion region.Using boundary condition $p_p(y = h_0)$ can be obtained as in Ref. [24]. h_0 is the height of depletion layer at any distance x under unbiased condition of the device. It can be written as,

$$h_0 = h(x)\big|_{(x=0, V_{gs}=0, V_{ds}=0)}. \tag{7}$$

1.1 Channel Potential distribution

Let $\varphi(x, y)$ be the 2D potential distribution of the channel. Now, $\varphi(x, y)$ can be determined by solving the following 2D Poisson's equation in the partially depleted channel region under the gate:

$$\frac{d^2\varphi(x,y)}{dx^2} + \frac{d^2\varphi(x,y)}{dy^2} = -\frac{qN_D(y)}{\varepsilon_s}, \tag{8}$$

where ε_s is the dielectric permittivity of GaAs semiconductor and q is electron charge.

We can use the following boundary conditions for solving Eq.(10):

$$\varphi(x, 0) = V_{bi} - V_{gs} - V_{op} \tag{9}$$

$$\varphi(0, y) = V_{bi} \tag{10}$$

$$\varphi(L, y) = V_{bi} + V_{ds} \tag{11}$$

$$\left.\frac{\partial\varphi(x,y)}{\partial y}\right|_{y=h_x} = 0 \tag{12}$$

where V_{bi} is the Schottky-barrier built-in potential, V_{gs} is the applied gate bias and V_{op} is the photovoltage developed at the Schottky junction due to illumination.

The solution of 2D Poisson's equation $\varphi(x, y)$ can be expressed using superposition technique [26] as:

$$\varphi(x,\ y) = \varphi_{1D}(y) + \varphi_{2D}(x,\ y), \tag{13}$$

where, $\varphi_{1D}(y)$ is 1D potential function of the long-channel MESFETs and $\varphi_{2D}(x,\ y)$ is the 2D potential function responsible for the short channel effects.

Following the method used by the Kabra et al. [27], the long channel potential function ($\varphi_{1D}(y)$) and the short channel potential function ($\varphi_{2D}(x,\ y)$) can be expressed as

$$\varphi_{1D}(y) = \frac{q\left(\sigma\sqrt{2}\right)^2}{\varepsilon_s}\left[-\frac{R\tau_p}{a}\left(\frac{y-R_p}{\sqrt{2}\sigma}\right)^2 + \frac{\Phi_o\tau_n \exp\left(-\alpha R_p\right)\exp\left(-\alpha\left(y-R_p\right)\right)}{\alpha\left(\sigma\sqrt{2}\right)} + \right.$$
$$+\frac{N_s}{2}\left(\frac{y-R_p}{\sqrt{2}\sigma}\right)^2 + c_c\left(N_p-N_s\right)\exp\left\{-\left(a_c\left(\frac{y-R_p}{\sqrt{2}\sigma}\right)+b_c\left(\frac{y-R_p}{\sqrt{2}\sigma}\right)^2\right)\right\} +$$
$$\left. +A\left(\frac{y-R_p}{\sqrt{2}\sigma}\right)+B\right] \tag{14}$$

where A, B are the arbitrary constants expressed as

$$A = -\frac{q\sigma\sqrt{2}}{\varepsilon_s}\left[-\left(a_c + 2b_c\left(\frac{h(x)-R_p}{\sqrt{2}\sigma}\right)\right)\exp\left[-\left(a_c\left(\frac{h(x)-R_p}{\sqrt{2}\sigma}\right)+b_c\left(\frac{h(x)-R_p}{\sqrt{2}\sigma}\right)^2\right)\right]\right.$$
$$\times c_c\left(N_p-N_s\right)+N_s\left(\frac{h(x)-R_p}{\sqrt{2}\sigma}\right)-R\tau_p a^{-1}\left(\frac{h_x-R_p}{\sqrt{2}\sigma}\right)-$$
$$\left.-\frac{\Phi_o\tau_n\exp\left(-\alpha R_p\right)\exp\left(-\alpha\left(h_x-R_p\right)\right)}{\left(\alpha\sigma\sqrt{2}\right)}\right], \tag{15}$$

$$B = -\left[\frac{N_s}{4}\left(\frac{-R_p}{\sigma}\right)^2 - \frac{R\tau_p}{2a}\left(\frac{-R_p}{\sigma}\right)^2 + c_c\left(N_p-N_s\right)\exp\left[-\left(a_c\left(\frac{-R_p}{\sqrt{2}\sigma}\right)+b_c\left(\frac{-R_p}{\sqrt{2}\sigma}\right)^2\right)\right]\right.$$
$$\left.+\frac{\Phi_o\tau_n\exp\left(-\alpha R_p\right)\exp\left(\alpha R_p\right)}{\alpha\left(\sigma\sqrt{2}\right)}+A\left(\frac{-R_p}{\sqrt{2}\sigma}\right)-q^{-1}\left(\sigma\sqrt{2}\right)^{-2}\varepsilon_s\left(V_{bi}-V_{gs}-V_{op}\right)\right]. \tag{16}$$

$$\varphi_{2D}\left(x,y\right) = \sum_{n=1}^{\infty}\frac{\sin(k_n y)}{\sinh(k_n L)}\left\{A_n\sinh[k_n(L-x)]+B_n\sinh(k_n x)\right\}, \tag{17}$$

where

$$k_n = (2n+1)\pi/[2h(x)] \tag{18}$$

$$A_n = \left(C_{1n}-C_{2n}-C_{3n}+C_{4n}-C_{5n}+C_{6n}+C_{7n}\right)M_n^{-1} \tag{19}$$

$$B_n = \left(C_{1n}+C_{11n}-C_{2n}-C_{3n}+C_{4n}-C_{5n}+C_{6n}+C_{7n}\right)M_n^{-1} \tag{20}$$

$$C_{1n} = -q\left(\sigma\sqrt{2}\right)^3 c_c(N_p-N_s)\varepsilon_s^{-1}k_n^{-3}\left[2b_c+k_n^2+-2b_c k_n^2\cos\left(k_n h\left(x\right)\right)+\right.$$

$$+\left(h(x)\left(a_c+b_c h(x)-1\right)k_n^2\cos\left(k_n h(x)\right)-\left(a_c+2b_c h(x)\right)k_n\right)\sin\left(k_n h(x)\right)\Big] \quad (21)$$

$$C_{11n}=\left(V_{ds}-V_{ds}\cos k_n h(x)\right)k_n^{-1} \quad (22)$$

$$C_{2n}=0.5q\left(\sigma\sqrt{2}\right)^3\varepsilon_s^{-1}k_n^{-3}N_s\Big[-2+\left(2-h(x)^2k_n^2\right)\cos\left(h(x)k_n\right)+$$
$$+2h(x)k_n\cos\left(h(x)k_n\right)\Big] \quad (23)$$

$$C_{3n}=q\left(\sigma\sqrt{2}\right)\ \Phi_o\tau_n\alpha^{-1}\exp\left(-\alpha R_p\right)\exp\left(-\alpha\sigma\sqrt{2}h(x)\right)\times$$
$$\times\left[\frac{k_n\exp\left(\alpha\sigma\sqrt{2}h(x)\right)-k_n\cos\left(h(x)k_n\right)-\alpha\sigma\sqrt{2}\sin\left(h(x)k_n\right)}{\alpha\left(\sigma\sqrt{2}\right)^2+k_n^2}\right]-$$
$$-\left(\frac{V_{bi}-V_{bi}\cos k_n h(x)}{k_n}\right) \quad (24)$$

$$C_{4n}=\frac{0.5q\left(\sigma\sqrt{2}\right)^3R\tau_p}{h(x)\varepsilon_s k_n^3}\times$$
$$\times\left[-2+\left(2-h(x)^2k_n^2\right)\cos\left(h(x)k_n\right)+2h(x)k_n\cos\left(h(x)k_n\right)\right] \quad (25)$$

$$C_{5n}=\frac{A\left(q\left(\sigma\sqrt{2}\right)^2\right)^2\left(-h(x)k_n\cos\left(h(x)k_n\right)+\sin\left(h(x)k_n\right)\right)}{k_n^2\varepsilon_s{}^2}+$$
$$+\frac{-R_pAq^2\left(\sigma\sqrt{2}\right)^4\left(-1+\cos\left(h(x)k_n\right)\right)}{\sigma\sqrt{2}k_n\varepsilon_s{}^2} \quad (26)$$

$$C_{6n}=q^2\left(\sigma\sqrt{2}\right)^6c_c\left(N_p-N_s\right)\varepsilon_s{}^{-2}k_n^{-1}\left(\left(a_c+2b_c\left(\frac{h(x)-R_p}{\sigma\sqrt{2}}\right)\right)^2-2b_c\right)\times$$
$$\times\exp\left(-a_c\left(\frac{h(x)-R_p}{\sigma\sqrt{2}}\right)-b_c\left(\frac{h(x)-R_p}{\sigma\sqrt{2}}\right)^2\right)\left(-1+\cos\left(h(x)k_n\right)\right) \quad (27)$$

$$C_{7n}=q\left(\sigma\sqrt{2}\right)^2\varepsilon_s{}^{-2}\left(\frac{1-\cos k_n h(x)}{k_n}\right)\Bigg[c_c\left(N_p-N_s\right)\exp\left[-\left(a_c\left(\frac{-R_p}{\sqrt{2}\sigma}\right)+b_c\left(\frac{-R_p}{\sqrt{2}\sigma}\right)^2\right)\right]+$$
$$+\frac{N_s}{2}\left(\frac{-R_p}{\sqrt{2}\sigma}\right)^2-\frac{R\tau_p}{a}\left(\frac{-R_p}{\sqrt{2}\sigma}\right)^2+\frac{\Phi_o\tau_n\exp\left(-\alpha R_p\right)\exp\left(\alpha R_p\right)}{\alpha\left(\sigma\sqrt{2}\right)^2}\Bigg]-$$

$$-\left(V_{bi}-V_{gs}-V_{op}\right)\left(\frac{1-\cos k_n h\left(x\right)}{k_n}\right) \tag{28}$$

$$M_n=\frac{1}{2}\left[h\left(x\right)-\frac{\sin\left(2h\left(x\right)k_n\right)}{2k_n}\right] \tag{29}$$

$\varphi(x, y)$ can be obtained by using the expressions of $\varphi_{1D}(y)$ and $\varphi_{2D}(x, y)$ from Eqs.(14) and Eq. (17) in Eq.(13), respectively. As Eq.(17) is an infinite series hence it is not possible to use it for computing the value of $\varphi_{2D}(x, y)$. Since, $\sinh[k_n(L-x)]$, $\sinh(k_nL)$, A_n and B_n are also decreased with the increase in n. Thus only the fundamental term ($n = 1$) is used to express $\varphi(x, y)$ as

$$\varphi\left(x,y\right)\approx\varphi_{1D}(y)+\frac{\sin(k_1y)}{\sinh(k_1L)}\left\{A_1\sinh[k_1(L-x)]+B_1\sinh(k_1x)\right\} \tag{30}$$

Where k_1, A_1, and B_1 can be determined by using $n = 1$ in Eq. (18), (19) and (20) respectively. Channel potential $\varphi_{ch}(x)$ can be given by

$$\varphi_{ch}\left(x\right)=\varphi\left(x,y\right)\Big|_{y=h(x)} \tag{31}$$

Where depletion region width is obtained by solving Eq.(29) and Eq.(30) under certain approximations as

$$h\left(x\right)=\left(\frac{qN_s}{\varepsilon_s}\right)^{-1}\left[-\left(D_1+D_2-2R_p\right)-\right.$$
$$\left.\left(\left(D_1+D_2-2R_p\right)^2+\frac{2qN_s}{\varepsilon_s}\left(\varphi_{ch}\left(x\right)+D-V_{bi}+V_{gs}+V_{op}\frac{D_1}{k_n}+\frac{D_2}{k_n}-\frac{qN_sR_p^2}{2\varepsilon_s}\right)\right)^{\frac{1}{2}}\right] \tag{32}$$

Where D, D_1 and D_2 can be given as.

$$D_1=\frac{\sinh[k_1(L-x)]\left(-2V_{bi}+V_{gs}+V_{op}-D\right)}{\sinh(k_1L)} \tag{33}$$

$$D_2=\frac{\sinh(k_1x)\left(-2V_{bi}+V_{gs}+V_{op}-V_{ds}-D\right)}{\sinh(k_1L)} \tag{34}$$

$$D=q\left(\sigma\sqrt{2}\right)^2\varepsilon_s^{-1}\left[c_c\left(N_p-N_s\right)\exp\left[-\left(a_c\left(\frac{-R_p}{\sqrt{2}\sigma}\right)+b_c\left(\frac{-R_p}{\sqrt{2}\sigma}\right)^2\right)\right]+\frac{N_s}{2}\left(\frac{-R_p}{\sqrt{2}\sigma}\right)^2-\right.$$
$$\left.R\tau_pa^{-1}\left(\frac{-R_p}{\sqrt{2}\sigma}\right)^2+\Phi_o\tau_n\alpha^{-1}\left(\sigma\sqrt{2}\right)^{-2}\exp\left(-\alpha R_p\right)\exp\left(\alpha R_p\right)\right] \tag{35}$$

2. RESULTS AND DISCUSSION

In this section, we will compare our model results with those obtained by using the commercially available 2D device simulator ATLAS™. The values of the parameters used for computation of the model results are: a = 0.2 μm, Z = 1 μm, L = 0.3 μm, V_{bi} = 1.01 V, R_p = 0.1 μm, σ = 0.02 μm, $N_p = 4 \cdot 10^{23}$ m^{-3}, T_m = 0.9 and $N_s = 10^{21}$ m^{-3}. The channel potential variation as a function of channel length (L) has been shown in Figs. 2(a)-(c) for different peak con-

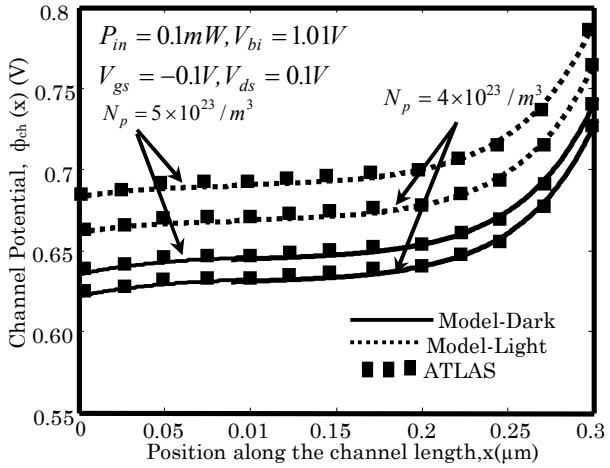

Fig. 2 (a) *– Variation of channel potential ($\varphi_{ch}(x)$) along the channel length for different peak doping concentration (N_p) in dark and illuminated conditions*

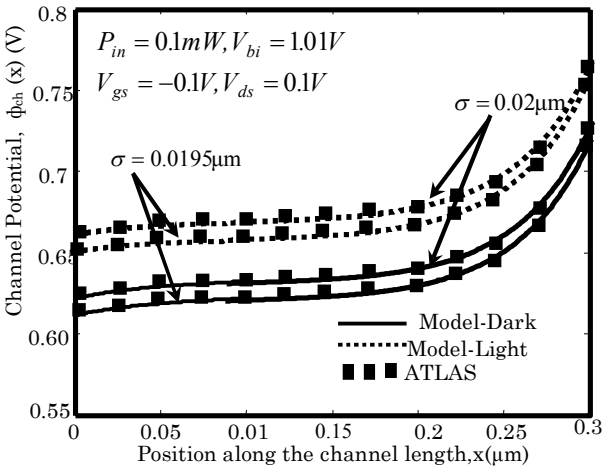

Fig. 2 (b) *– Variation of channel potential ($\varphi_{ch}(x)$) along the channel length for different straggle parameter (σ_p) in dark and illuminated conditions*

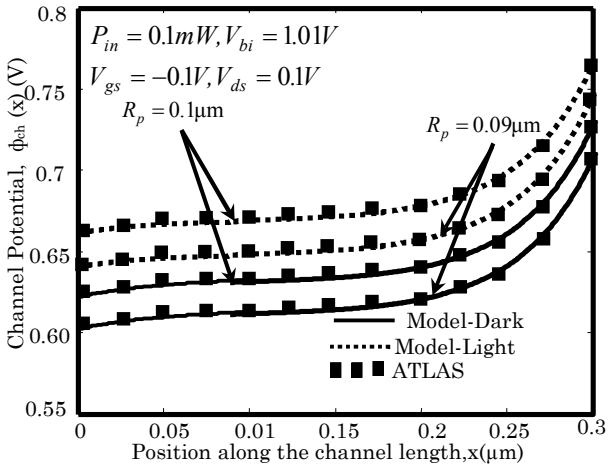

Fig. 2(c) *– Variation of channel potential($\varphi_{ch}(x)$) along the channel length for different projected range (R_p) in dark and illuminated conditions*

centration (N_p), straggle parameter (σ_p) and projected range (R_p) of the doping profile. It is observed that source-channel barrier height is decreased with the increase in the value of N_p, R_p and σ_p, due to the increase in the average implanted ion density in the active channel region of the MESFET with the increase in above profile parameters under both dark and illuminated condition. It is also evident from the Figs. 2(a)-(c) that for a given gate length, the source-channel barrier height is reduced due to the incident optical radiation on the device. This is due to the fact that the photovoltage developed across the junction due to illumination forward biases the Schottky gate-channel junction and thereby decreasing the source-channel barrier height.

3. CONCLUSION

In this paper, analysis of short gate length GaAs MESFET with a Gaussian-like doping profile in the vertical direction has been done under dark and illumination. The 2D potential distribution has been derived by solving the 2D Poisson's equation using the separation of variable technique. The proposed model results are found to be well-matched with the ATLAS™ simulation data verifying the validity of the model. This model can be well-implemented in design of photonic MMICs.

REFERENCES

1. I.J. Bahl, *IEEE Microw. Wirel. Co.* **18**, 52 (2008).
2. I.J. Bahl, D. Conway, *IEEE T. Microw. Theory* **56**, 293 (2008).
3. J.A. Torres, J.C. Freire, *IEEE T. Microwave Theory* **50**, 51 (2002).
4. F. Ellinger, R. Vogt, *IEEE Microw. Wirel. Co.* **11**, 104 (2001).
5. C.H. Lee, S. Han, *IEEE Microw. Guided W.* **10**, 325 (2000).
6. T.L. Nguyen, A.P. Freundorfer, *IEEE Photonics Tech. Lett.* **9**, 499 (1997).

7. J.M. Zamanillo, J. Portilla, C. Navarro, C. Perez-Vega, *Proceedings of 35th European Microwave Conference (EuMC)*, 1391 (2005).
8. S. Bose, M. Gupta, R.S. Gupta, *Microwave Opt. Technol. Lett.* **26**, 279 (2000).
9. S. Bose, Adarsh R.S. Gupta, *Appl. Microwave Wireless* **13**, 68 (2001).
10. J. Rodriguez-Tellez, K.A. Mezheg, N.T. Ali, T. Fernandei, A. Mediavilla, A. Tazon, C. Navarro, *Proceedings of 10th International Conference on Electronics, Circuits & Systems (ICECS)*, 970 (2003).
11. V.K. Singh, S.N. Chattopadhyay, B.B. Pal, *Solid State Electron.* **29**, 707 (1986).
12. S. Mishra, V.K. Singh, B.B. Pal, *IEEE T. Electron. Dev.* **37**, 2 (1990).
13. P. Chakrabarti, A. Gupta, N.A. Khan, *Solid-State Electron.* 39, 1481 (1996).
14. S. Bose, Adarsh, Ritesh Gupta, Mridula Gupta, R.S. Gupta, *Microwave Opt. Technol. Lett.* **32**, 138 (2002).
15. B.K. Mishra, Lochan Jolly, Kalawati Patil, *International journal of VLSI design & Communication Systems (VLSICS)* **23**, 1 (2010).
16. S.N. Mohammad, M.B. Patil, J.I. Chyi, G.B. Gao, H. Morkoc, *IEEE T. Electron. Dev.* **37**, 11 (1990).
17. C.H. Liu, L.W. Wu, S.J. Chang, J.F. Chen, U.H. Liaw, S.C. Chen, *J. Mater. Sci.: Mater El.* **15**, 91 (2004).
18. A. Dasgupta, S.K. Lahiri, *Int. J. Electron.* **61**, 655 (1986).
19. ATLAS: Silvaco International 2008.
20. S.A. Bashar *Study of Indium Tin Oxide (ITO) for Novel Optoelectronic Devices*, PhD Thesis, (King's College of London, University of London: 1998).
21. S.M. Sze, *Physics of semiconductor devices*, (New York: Wiley: 1981).
22. A. Dasgupta, S.K. Lahiri, *IEEE T. Electron Dev.* **35**, 390 (1988).
23. S. Bose, M. Gupta, R.S. Gupta, *Microelectron. J.* **32**, 241 (2001).
24. S. Jit, B.B. Pal, *IEEE T. Electron. Dev.* **48**, 2732 (2001).
25. E. Kreyszig, *Advanced Engineering Mathematics* (New York: Wiley: 1993).
26. K.N. Ratnakumar, J.D. Meindel, *IEEE J. Solid State Circuits* **17**, 937 (1982).
27. S. Kabra, H. Kaur, S. Haldar, M. Gupta, R.S. Gupta, *Microelectron. J.* **38**, 547 38 (2007).